

Coadministration of a Plasmid Encoding HIV-1 Gag Enhances the Efficacy of Cancer DNA Vaccines

Laure Lambricht¹, Kevin Vanvarenberg¹, Ans De Beuckelaer², Lien Van Hoecke^{2,3}, Johan Grooten², Bernard Ucakar¹, Pascale Lipnik⁴, Niek N Sanders^{5,6}, Stefan Lienenklaus^{7,8}, Véronique Prémat¹ and Gaëlle Vandermeulen¹

¹Advanced Drug Delivery and Biomaterials, Louvain Drug Research Institute, Université catholique de Louvain, Brussels, Belgium; ²Department of Biomedical Molecular Biology, Ghent University, Ghent, Belgium; ³VIB Medical Biotechnology Center, Ghent University, Ghent, Belgium; ⁴Bio and Soft Matter, Université catholique de Louvain, Louvain-La-Neuve, Belgium; ⁵Laboratory of Gene Therapy, Ghent University, Ghent, Belgium; ⁶Cancer Research Institute Ghent, Ghent, Belgium; ⁷Institute for Laboratory Animal Science, Hannover Medical School, Hannover, Germany; ⁸Institute for Experimental Infection Research, Centre for Experimental and Clinical Infection Research, TWINCORE, Hannover, Germany

DNA vaccination holds great promise for the prevention and treatment of cancer and infectious diseases. However, the clinical ability of DNA vaccines is still controversial due to the limited immune response initially observed in humans. We hypothesized that electroporation of a plasmid encoding the HIV-1 Gag viral capsid protein would enhance cancer DNA vaccine potency. DNA electroporation used to deliver plasmids *in vivo*, induced type I interferons, thereby supporting the activation of innate immunity. The coadministration of ovalbumin (OVA) and HIV-1 Gag encoding plasmids modulated the adaptive immune response. This strategy favored antigen-specific Th1 immunity, delayed B16F10-OVA tumor growth and improved mouse survival in both prophylactic and therapeutic vaccination approaches. Similarly, a prophylactic DNA immunization against the melanoma-associated antigen gp100 was enhanced by the codelivery of the HIV-1 Gag plasmid. The adjuvant effect was not driven by the formation of HIV-1 Gag virus-like particles. This work highlights the ability of both electroporation and the HIV-1 Gag plasmid to stimulate innate immunity for enhancing cancer DNA vaccine immunogenicity and demonstrates interesting tracks for the design of new translational genetic adjuvants to overcome the current limitations of DNA vaccines in humans.

Received 19 November 2015; accepted 9 June 2016; advance online publication 19 July 2016. doi:10.1038/mt.2016.122

INTRODUCTION

Harnessing the power of the immune system to treat or prevent diseases via vaccine administration is one of the most successful public health interventions. DNA vaccines consist of a recombinant antigen encoded by engineered DNA plasmids and are expressed *in vivo* to solicit immunity against pathogens or cancer cells.¹ DNA vaccines are promising for cancer immunotherapy as they induce a broad immune response,² including both a T helper

type 1 (Th1) response and cytotoxic T lymphocytes (CTLs), the most potent effectors against cancer cells.^{3,4} They also prime CD4+ T cells, thereby supporting the activity of CTLs and memory T cells.⁵ Currently, two DNA vaccines are licensed for veterinary use. Oncept (Merial, Lyon, France) is commercialized for the treatment of melanoma in dogs and Apex-IHN (Novartis, Basel, Switzerland) for prophylactic vaccination of salmon against infectious hematopoietic necrosis virus. Despite the commercial use of DNA vaccine in veterinary medicine, DNA vaccination is still under investigation for use in humans because the immunogenicity is often lower than other conventional vaccines.

In recent years, several advancements have been made to improve DNA vaccine immunogenicity in humans, leading to an increasing number of clinical trials.⁶ Particularly, plasmid delivery by *in vivo* electroporation (EP) and the use of genetically encoded immune adjuvants have enhanced DNA vaccine efficacy.⁷ First, EP is the most commonly used and the most powerful nonviral delivery method for DNA vaccines.^{6,8} This method was used to improve DNA vaccine efficacy in large animals.^{7,9} EP efficiency is not only attributed to an enhanced gene transfer⁷ but also to the induction of a transient tissue inflammation and the subsequent local recruitment of immune cells.^{1,10} Second, genetic adjuvants, *i.e.*, plasmid vectors encoding immunomodulatory molecules, aim at enhancing the immunogenicity of antigens *in vivo*. They stimulate the innate immune system to trigger appropriate dendritic cell (DC) maturation and thereby a robust, specific, and long-lasting adaptive immune response. Indeed, the type of insult that drives DC maturation affects whether and how a T cell will respond to an antigen, as T-cell priming, expansion, function, and localization are controlled by sequential signals provided by DCs.¹¹ These genetic adjuvants include cytokines, chemokines, or immune stimulatory molecules, such as toll-like receptor (TLR) agonists or interferon (IFN) regulatory factors.^{7,12–14} Most of these adjuvants are used in preclinical studies, and even though they are promising, only a few of them have been evaluated in clinical trials until now. Therefore, there is still a critical need of clinically applicable genetic adjuvants.

Correspondence: Véronique Prémat, Advanced Drug Delivery and Biomaterials, Louvain Drug Research Institute, Université catholique de Louvain, Avenue Mounier 73, bte B1.73.12, 1200 Brussels, Belgium. E-mail: veronique.preat@uclouvain.be

Plasmids encoding HIV-1 Gag (pGag) have been widely studied during the past decades in the context of HIV vaccine development. In clinical trials, their safety and immunogenicity have been demonstrated.^{15–17} The HIV-1 Gag proteins are able to self-assemble leading to virus-like particle (VLP) formation,¹⁸ and these capsid proteins may constitute a general pathogen-associated molecular pattern (PAMP) for innate sensing.¹⁹ Moreover, combining a gp160-encoding DNA vaccine with pGag enhanced the immune response to the gp160 envelop antigen of HIV-1,²⁰ thereby suggesting the pGag's adjuvant potential.

In this study, we hypothesize that the *in vivo* EP of pGag could enhance cancer DNA vaccine immunogenicity. First, we tested whether cell transfection with pGag led to subsequent VLP formation. Then, we analyzed whether EP induced innate immunity *in vivo*. The effects of pGag on the immune response against a model antigen (ovalbumin (OVA)) and a tumor-associated antigen (TAA) (gp100) were evaluated in B16F10-OVA melanoma. Finally, we evaluated whether the *in vivo* pGag immunomodulatory effects were mediated by the formation of VLPs.

RESULTS

Cell transfection with a plasmid coding for HIV-1 Gag leads to VLP formation *in vitro*

To assess whether cell transfection with the pGag vector encoding the full length and unmodified HIV-1 Gag protein would lead to the expression of HIV-1 Gag proteins and subsequent VLP formation, this plasmid was transfected by lipofection in HEK 293T cells *in vitro*. Particles isolated from the cell supernatant were characterized. After negative staining of the samples, spherical particles were observed under a transmission electron microscope (Figure 1a). Dynamic light scattering analyses showed a uniform population of particles with a size of 180 ± 1 nm and a polydispersity index of 0.06 ± 0.03 (mean \pm SD, $n = 3$) (Figure 1b). Finally, particle composition was assessed by Western blotting. The HIV-1 Gag protein was detected in the purified samples (Figure 1c).

Plasmid DNA EP induces type I IFN responses *in vivo*

Type I IFNs are antiviral cytokines endowed with many biological effects, including antitumor activity.²¹ The effect of EP on the induction of type I IFNs was assessed using IFN- β reporter mice in which a luciferase gene is placed under the control of the IFN- β promoter. Via *in vivo* bioluminescence imaging, the induction of IFN- β can be localized and quantified. EP applied after an injection of phosphate buffered saline (PBS) did not significantly stimulate IFN- β induction. The injection of an empty vector without EP induced a low type I IFN induction 24 hours after the injection, but only the combination of EP and an empty plasmid DNA (pDNA) vector strongly induced the IFN- β promoter (Figure 2a,b). The luciferase expression levels increased drastically during the first 6 hours then remained stable and started decreasing after 48 hours. IFN- β induction remained localized at the injection site (Figure 2b).

Codelivery of the HIV-1 Gag plasmid promotes the Th1 polarization of the immune response

To investigate the ability of the HIV-1 Gag plasmid to modulate the immune response, the OVA model antigen was initially

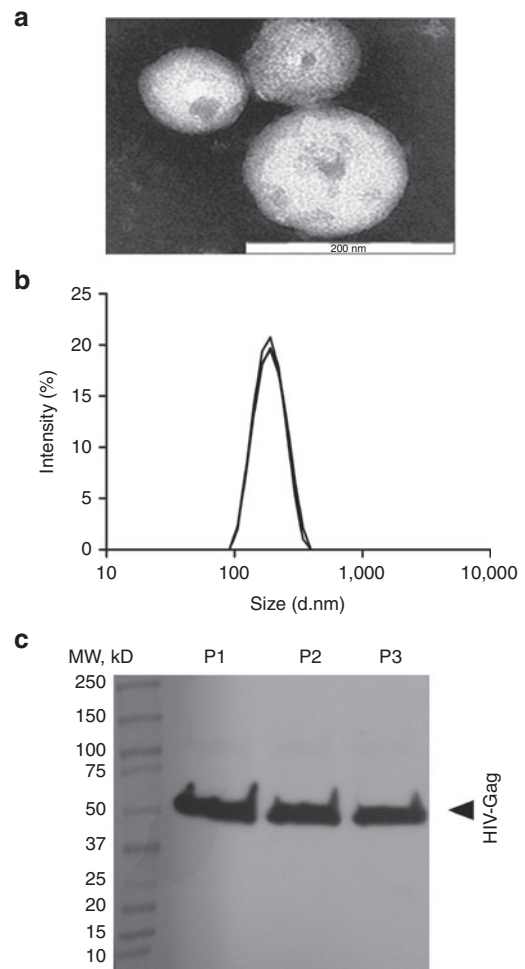


Figure 1 The characterization of HIV-1 Gag virus-like particles (VLPs). VLPs purified from the supernatants of HEK 293T cells transfected with HIV-1 Gag plasmid. (a) Particles observed by transmission electron microscopy after purification and negative staining of samples. This image is representative of data from three replicate experiments. Bare scale: 200 nm. (b) Individual measurement of particle size by DLS ($n = 3$). Particle size is calculated from the translational diffusion coefficient using the Stokes–Einstein equation. (c) Western blot analysis of three replicate productions of VLPs purified by ultracentrifugation (P1, P2, P3) with rabbit polyclonal antibodies to HIV-1 Gag as primary antibodies and polyclonal goat anti-rabbit immunoglobulins labeled with biotin as secondary antibodies. The HIV-1 Gag protein was detected at ~56 kDa.

chosen because it allows for both immune response characterization and tumor growth studies. Taking into account the high immunogenicity of OVA, mice were immunized with a low dose (1 μ g) of OVA encoding plasmid (pOVA). The same amount of pGag was codelivered with pOVA or not to determine if it would impact the immune response *in vivo*. After priming, blood samples analysis indicated that the humoral response remained very low while it slightly increased after the first and second boost (Figure 3a). The delivery of pOVA alone led to higher total anti-OVA antibody titers compared to mice where pGag was codelivered (Figure 3a). Analysis of immunoglobulins G1 and G2a showed that these lower antibody titers correlated with a shift of anti-OVA antibody isoforms toward IgG2a (Figure 3b). In mice immunized with both pOVA and pGag,

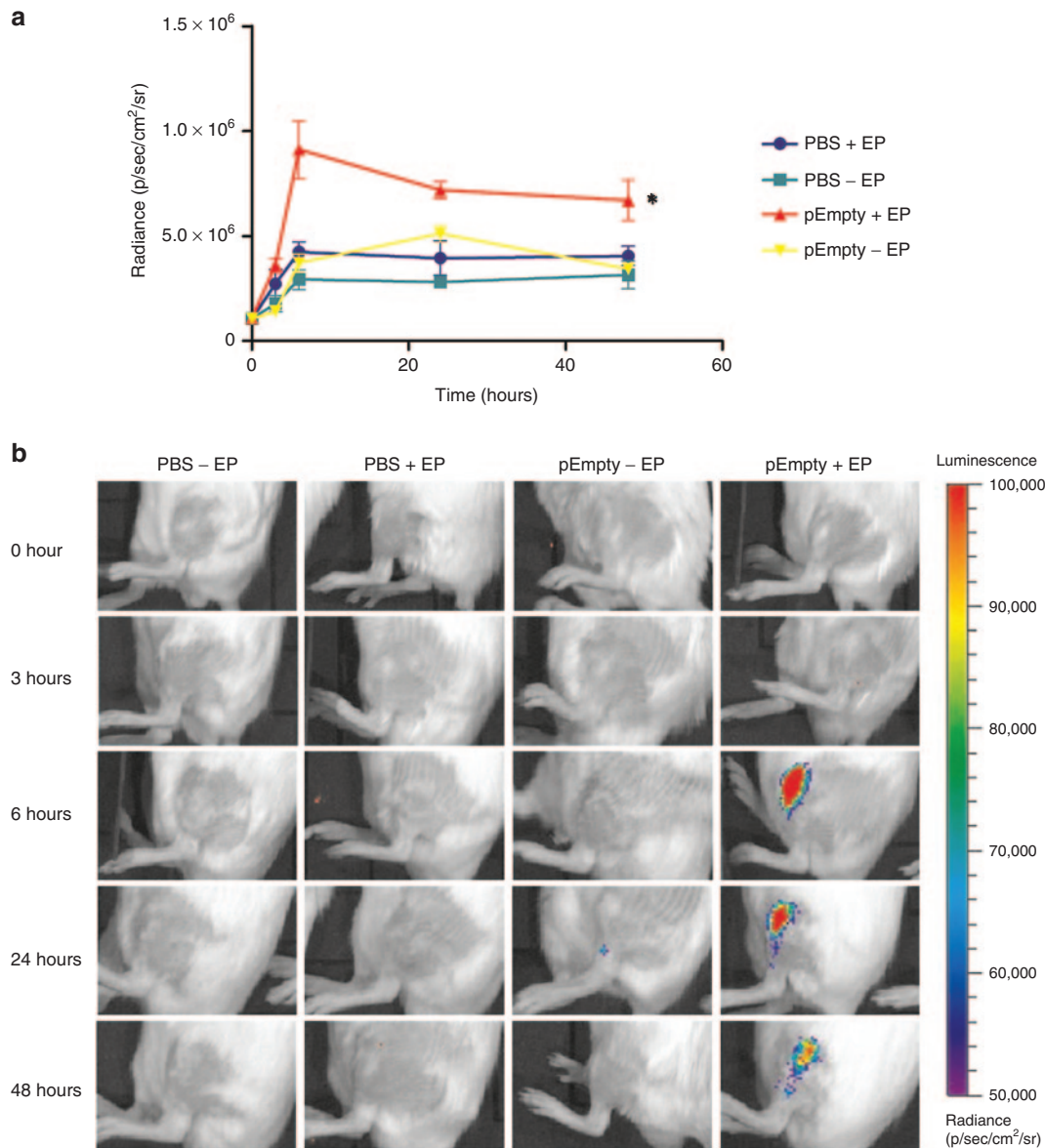


Figure 2 The effect of plasmid electroporation on type 1 interferon (IFN) expression. Groups of naive heterozygous luciferase reporter mice (IFN- β +/ Δ β -luc) were treated with phosphate buffered saline (PBS) or an empty plasmid (pEmpty) before applying eight 20 ms and 200V/cm electric pulses with plate electrodes (+EP) or not (-EP). Type 1 IFN expression was quantified by *in vivo* bioluminescence imaging following i.p. injection of luciferin. **(a)** Radiance was observed at 0, 3, 6, 24, and 48 hours following treatment. The results are presented as the mean \pm SEM ($n = 4$). The asterisks indicate significant differences compared to the control group PBS without EP ($*P < 0.05$) (Friedman test and Dunn's *post-hoc* test). **(b)** Representative imaging of the mice as a function of treatment and time. Color presentation indicates the intensity of bioluminescence, as shown in the bar.

the mean IgG2a/IgG1 ratio was 540 times higher than in mice immunized with pOVA alone. In addition, 2 weeks after the last boost, IFN- γ levels were analyzed at different time points following restimulation of splenocytes with OVA. Significantly higher IFN- γ concentrations were observed in the groups where pOVA was combined with pGag (Figure 3c). Finally, the codelivery of pGag tended to improve the cell-mediated acquired immune defense against cells expressing the vaccine antigen. Indeed, higher killing rate (P value: 0.09) of OVA-expressing target cells was observed in mice immunized with pGag and pOVA as compared to mice that received the DNA vaccine alone (Figure 3d).

Codelivery of the HIV-1 Gag plasmid during prophylactic anti-OVA DNA immunization delayed B16F10-OVA melanoma tumor growth

To explore if codelivery of pGag would effectively impact cancer DNA vaccine efficiency, mice were prophylactically immunized with 1 μ g pOVA combined or not with 1 μ g pGag. After challenge, tumor growth and mouse survival were followed (Figure 4a). The median survival in naive mice was 27 days, and no naive mice were alive after 56 days. Survival was significantly better in mice immunized with pOVA. The median survival time reached 54 days with a final survival ratio of 1/6 (Figure 4b). Importantly, the survival was far better in mice immunized with the combination of pOVA

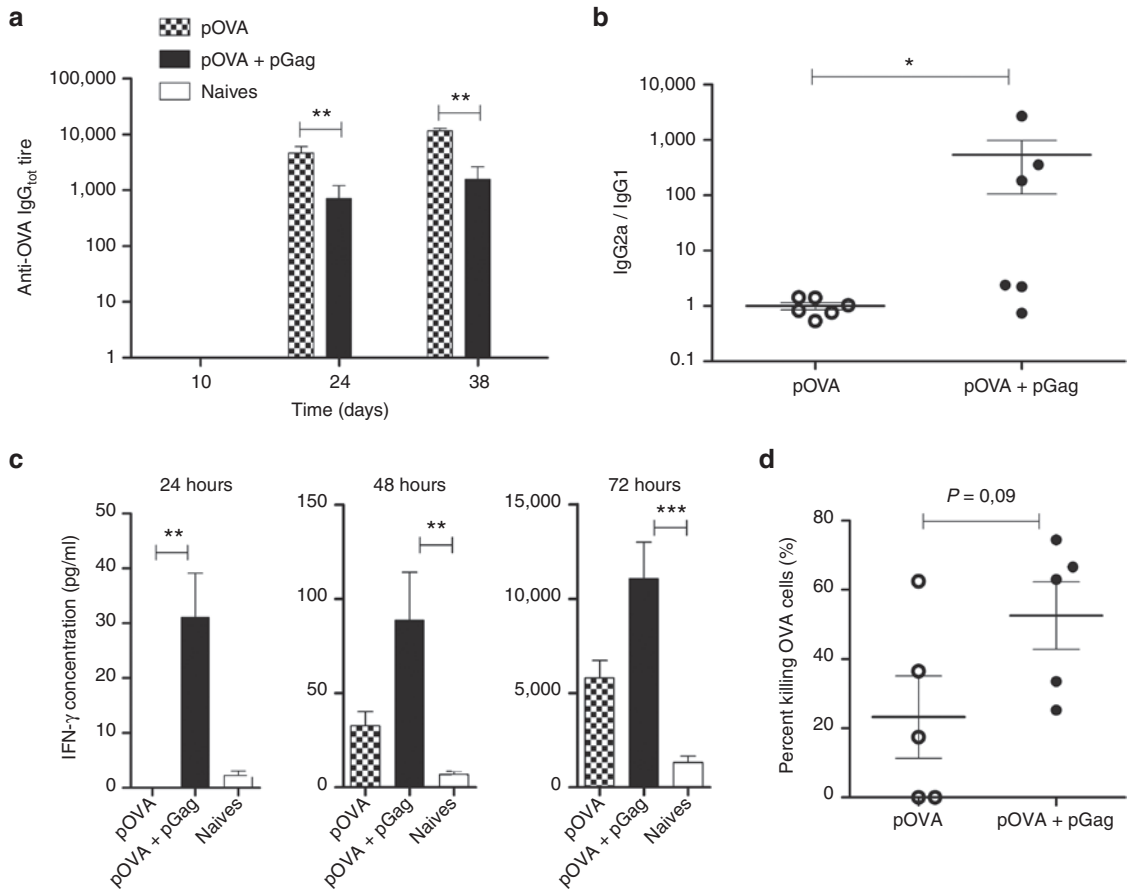


Figure 3 The effect of pGag codelivery during anti-ovalbumin (OVA) immunization on the immune response. C57BL/6 mice were immunized in a regimen of one prime and two boosts at a 2-week interval with the antigenic OVA plasmid combined or not with the HIV-1 Gag plasmid. **(a)** OVA-specific total IgG titers were measured by enzyme-linked immunosorbent assays (ELISAs) in the sera of mice collected at experimental days 10, 24, and 38 (10 days after each vaccine delivery, considering day 0 as the priming day). The error bars indicate mean \pm SEM ($n = 6$). The asterisks indicate significant differences between groups (** $P < 0.01$) (Mann-Whitney *U*-test and Bonferroni tests). **(b)** Antibody isotypes were analyzed in sera of mice randomly collected 10 days after the last boost. Individual IgG1 and IgG2a titers were measured by ELISAs and each mouse was characterized by an IgG2a/IgG1 ratio (* $P < 0.05$) (Mann-Whitney *U*-test). **(c)** To analyze OVA-specific IFN- γ levels, mice were immunized and sacrificed 1 week after the last vaccine administration. IFN- γ concentrations measured in the supernatant of mice splenocytes that had been restimulated with OVA protein 24, 48, and 72 hours before. The error bars indicate mean \pm SEM ($n = 6$). The asterisks indicate significant differences between groups (** $P < 0.01$, *** $P < 0.001$) (Kruskal-Wallis and Dunn's *post-hoc* test). **(d)** The percentage of antigen-specific killing was analyzed by *in vivo* cytotoxic assay. Immunized mice were adoptively transferred with two populations of labeled splenocytes: MHC-I OVA peptide-pulsed-target cells and a MHC-I irrelevant-peptide-pulsed cells. Two days after transfer, the specific killing of target cells was obtained by comparing the relative decrease of the two populations. Percentages of OVA target cell killing were compared using the Mann-Whitney *U*-test.

and pGag. In that case, the median survival was 83 days and half of the mice were still alive at the end of the experiment. The tumor volume as a function of time profile shows that vaccination strongly delayed tumor growth (Figure 4c). Tumor volumes were significantly lower in vaccinated mice compared to naives, and the size was smaller in mice immunized with the two plasmids, with significant differences observed from day 26 to 70. No progression of the implanted tumor was observed in mice immunized with pOVA combined with pGag for more than 2 weeks longer than mice immunized with the pOVA DNA vaccine alone. The mean tumor size reached 500 mm³ 23 days later in the group immunized with the two plasmids, compared to mice immunized with pOVA alone.

Codelivery of the HIV-1 Gag plasmid during prophylactic anti-gp100 DNA immunization delayed B16F10-OVA melanoma tumor growth

Next, the ability of pGag to improve DNA vaccine effectiveness in the case of less immunogenic TAA was assessed. Prophylactic immunization with 50 μ g of a plasmid coding for the gp100 melanoma antigen (pGP100) combined or not with 1 μ g pGag was performed before challenging the mice (Figure 5a). Tumor growth was slower when pGag was codelivered with pGP100 (Figure 5c). At day 14 after challenge, the implanted tumor was still not visible in four out of the six mice when the pGP100 vaccine was codelivered with pGag, while only two out of six mice did not display progression of the tumor implanted when

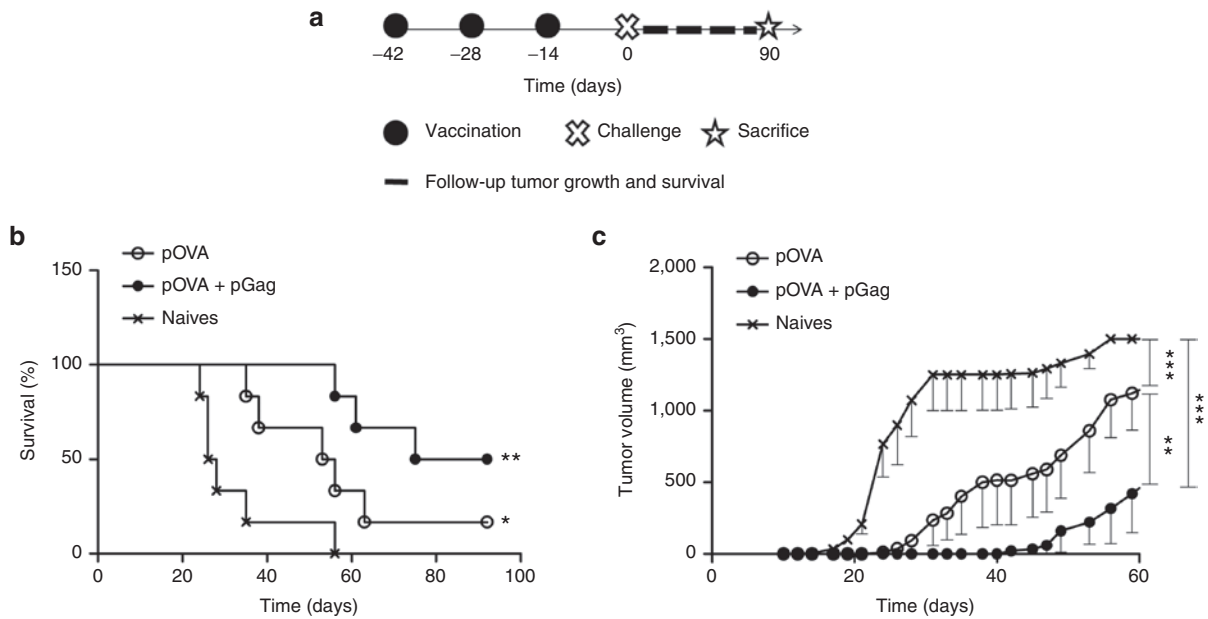


Figure 4 The effect of pGag codelivery during prophylactic anti-ovalbumin (OVA) immunization on the antitumor activity. **(a)** Experimental plan. C57BL/6 mice were immunized in a regimen of one prime and two boosts at a 2-week interval with the antigenic OVA plasmid combined or not with pGag. Two weeks after the last vaccination, they were challenged with B16F10-OVA cells. Tumor growth and mouse survival were assessed for 3 months. **(b)** Survival rates monitoring after challenge. The asterisks indicate significant differences compared with naive mice ($*P < 0.05$, $**P < 0.01$) (comparison of survival curves, Mantel–Cox test). **(c)** Tumor growth follow-up after challenge in mice immunized with pOVA and pOVA combined with pGag. The results are expressed as mean – SEM ($n = 6$). The asterisks show significant differences between groups ($**P < 0.01$, $***P < 0.001$) (analysis of variance, Dunnett’s *post-hoc* test).

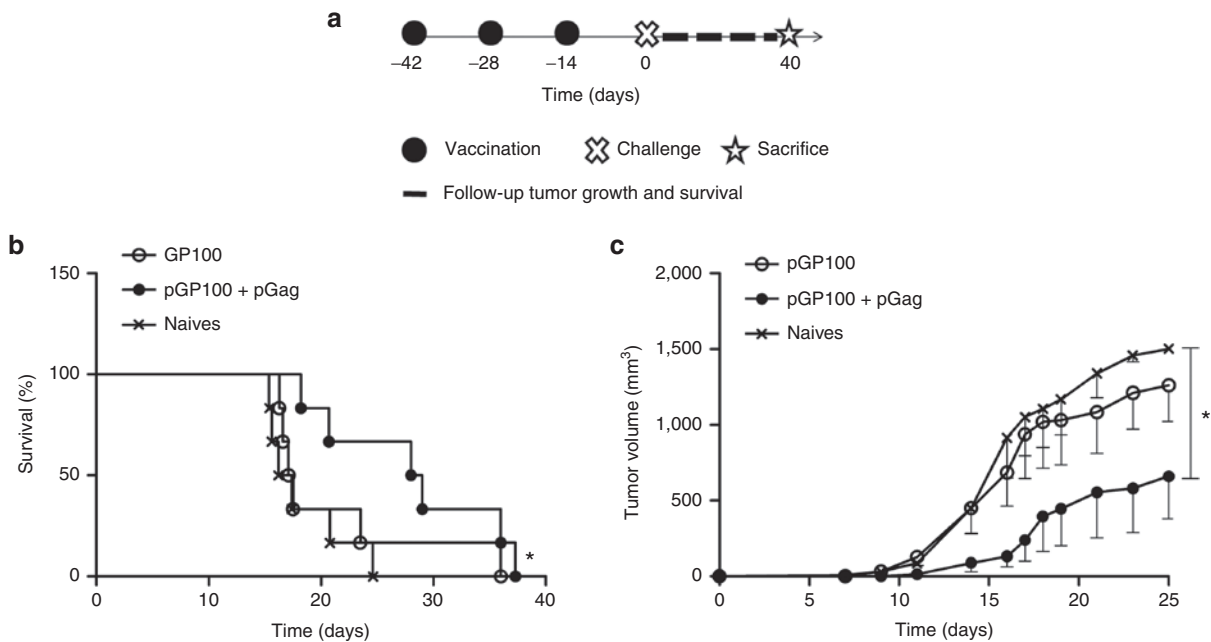


Figure 5 The effect of pGag codelivery during prophylactic anti-GP100 immunization on the antitumor activity. **(a)** Experimental plan. C57BL/6 mice were immunized in a regimen of one prime and two boosts at a 2-week interval with the antigenic GP100 plasmid combined or not with pGag. Two weeks after the last vaccination, they were challenged with B16F10-OVA cells and tumor growth and mouse survival were monitored. **(b)** Survival rates monitoring after challenge. The asterisks indicate significant differences compared with naive mice ($*P < 0.05$) (comparison of survival curves, Mantel–Cox test). **(c)** Tumor growth follow-up after challenge in mice immunized with pGP100 and pGP100 combined with pGag. The results are expressed as mean – SEM ($n = 6$). The asterisks show significant differences between groups ($*P < 0.05$) (analysis of variance, Dunnett’s *post-hoc* test).

mice were immunized with pGP100 alone. All tumors were growing in naive mice at that time. Additionally, 3 weeks after challenge the mean tumor volume in the pGP100 and pGag immunized mice was lower ($555 \text{ mm}^3 \pm 301$) (mean \pm SEM, $n = 6$) than in the pGP100 immunized ($1,083 \text{ mm}^3 \pm 270$; $P = 0.2$) and naive ($1,339 \text{ mm}^3 \pm 161$; $P = 0.04$) mice. Survival curves confirmed the positive effect of pGag (Figure 5b), as a significant improvement in survival was visible following pGag codelivery, whereas no significant difference was observed in the case of the gp100-encoding plasmid delivered alone.

Codelivery of the HIV-1 Gag plasmid during therapeutic anti-OVA DNA immunization delayed B16F10-OVA melanoma tumor growth

Finally, the therapeutic potential of a DNA vaccine combined or not with pGag was evaluated. To evaluate such a therapeutic effect, the pOVA DNA vaccine was selected. The low immunogenicity of the pGP100 plasmid and the rapid growth of B16F10-OVA tumors predicted a poor efficiency of a gp100 therapeutic DNA vaccine. As therapeutic immunization consists of vaccine administration after the disease onset, the treatment started 2 days after the implantation of B16F10-OVA tumors (Figure 6a) and consisted of $1 \mu\text{g}$ of pOVA with or without $1 \mu\text{g}$ pGag. The mix of pOVA and pGag significantly delayed tumor growth (Figure 6c). Indeed, it took 17 days for tumors to reach 500 mm^3 in mice immunized with pOVA and 24 days when pGag was added. At day 21, the mean tumor volume (\pm SEM) was $217 \pm 68 \text{ mm}^3$, $703 \pm 228 \text{ mm}^3$, and $989 \pm 208 \text{ mm}^3$ with 90%, 56%, and 40% of tumors that were smaller than 500 mm^3 for mice treated with the combination of pOVA and pGag, with pOVA alone and for nonimmunized mice, respectively. Mouse survival was also significantly increased when

pGag was codelivered (Figure 6b). These results demonstrate that therapeutic DNA immunization with pOVA codelivered with pGag, but not with pOVA alone, promoted tumor growth delay.

The formation of HIV-1 Gag VLPs is not required for adjuvant immunomodulatory effect

To assess whether the adjuvant effect of pGag could be mediated by the formation of VLPs, a plasmid encoding a mutated version of HIV-1 Gag (pGag*) was constructed. pGag* encoded a protein very close in sequence to the native Gag protein, but three specific points mutations make it neither able to bind to the plasma membrane, nor to self-assemble properly in VLP.²² First, a prophylactic immunization experiment followed by a tumor challenge (Figure 5a) demonstrated that pGag and pGag*, when combined to pOVA, had the same effect on tumor growth (Figure 8a–c). The same conclusion was drawn from the therapeutic immunization experiments as the combination of pOVA with pGag or pGag* was equally efficient (Figure 7a–c). This suggests that the adjuvant role of pGag on the vaccine-antigen specific immune response is probably not mediated by the formation of HIV-1 Gag VLPs *in vivo*. Interestingly, EP of pGag or pGag* alone had a delaying impact on tumor growth during therapeutic (Figure 7a,c) but not prophylactic (Figure 8a,c) immunizations. This result further supports the role of Gag encoding plasmid as a stimulator of the innate immune system.

DISCUSSION

Despite promising results in animal models, the clinical efficacy of DNA vaccines remains to be proven due to the weakness of the immune response observed in humans. There is therefore a critical need to find new strategies to enhance DNA vaccine

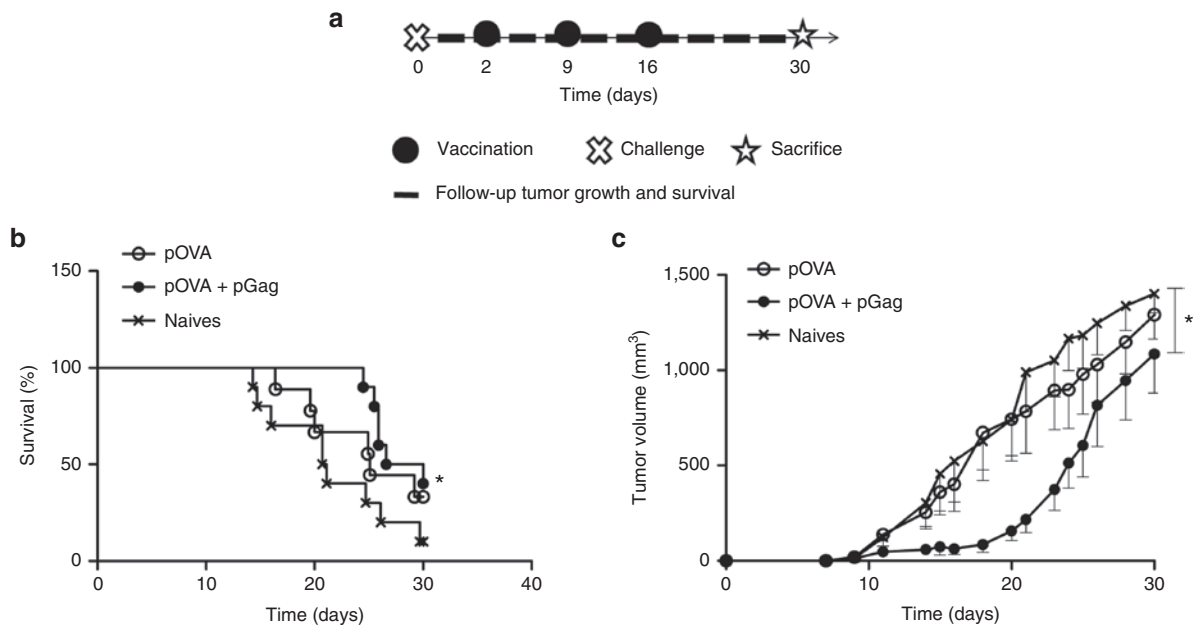


Figure 6 The effect of pGag codelivery during therapeutic anti-ovalbumin (OVA) immunization on the antitumor activity. **(a)** Experimental plan. C57BL/6 mice were challenged with B16F10-OVA cells. Two days later, they were immunized in a regimen of one prime and two boosts at a 1-week interval with the antigenic OVA plasmid combined or not with HIV-1 Gag plasmid. Tumor growth and mouse survival were assessed after challenge. **(b)** Survival rates monitoring after challenge. The asterisks indicate significant differences compared with naive mice ($*P < 0.05$) (comparison of survival curves, Mantel–Cox test). **(c)** Tumor growth follow-up after challenge in mice immunized with pOVA and pOVA combined with pGag. The results are expressed as mean \pm SEM ($n = 10$). The asterisks show significant differences between groups ($*P < 0.05$) (analysis of variance, Dunnett's *post-hoc* test).

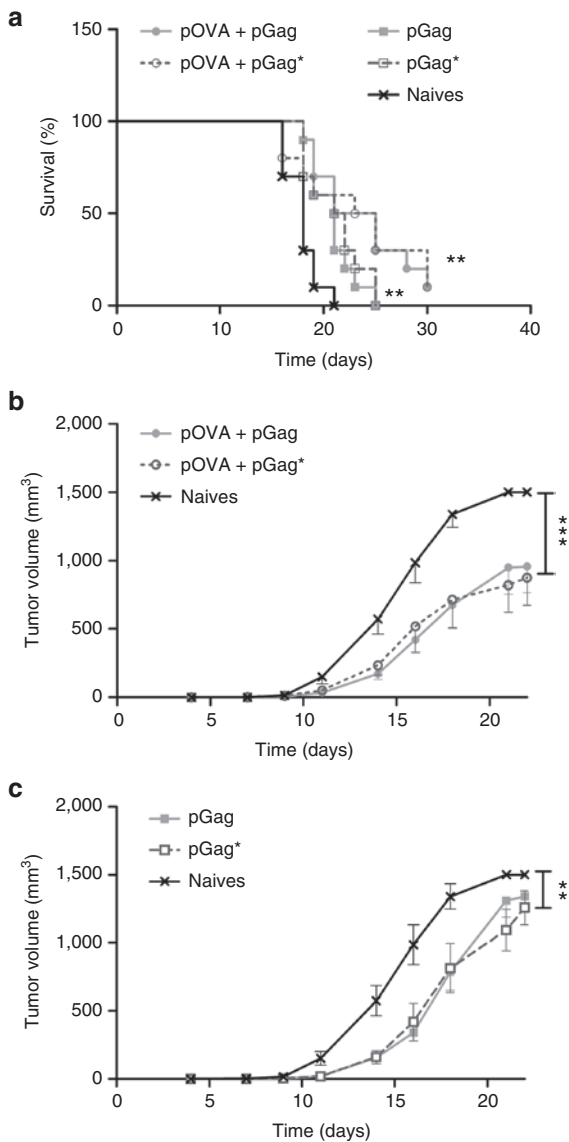


Figure 7 Comparison of the effect of pGag and pGag* during therapeutic anti-ovalbumin (OVA) immunization on the antitumor activity. **(a)** Survival rate monitoring after challenge. The asterisks indicate significant differences compared with naive mice (** $P < 0.01$) (comparison of survival curves, Mantel–Cox test). **(b,c)** Tumor growth follow-up after challenge in mice immunized respectively with pOVA combined with pGag or pGag* and mice immunized with pGag or pGag* alone. The results are expressed as mean \pm SEM ($n = 10$). The asterisks show significant differences between groups (** $P < 0.01$, *** $P < 0.001$) (analysis of variance, Dunnett's *post-hoc* test).

immunogenicity and to have them train the immune system to generate potent immune responses. As EP and the use of genetic adjuvants were shown previously to enhance DNA vaccine efficacy, we investigated whether the EP of a plasmid encoding the HIV-1 Gag protein could increase cancer DNA vaccine immunogenicity. We showed that codelivery of pGag by EP enhanced the potency of the immune response against the vaccine antigens, suggesting a strong adjuvant effect of this strategy.

Firstly, we showed that cell transfection with pGag led to the production of VLPs by the cellular machinery. This result was expected as HIV-1 Gag proteins are responsible for viral capsid

assembly.¹⁸ These particles are similar in size, composition, and structure to intact infectious virus (Figure 1a–c). Nevertheless, they do not present any infectivity risk as they are devoid of the viral genome.²³ Several studies have been highlighting the immunomodulatory properties of HIV-1 Gag proteins. On the one hand, HIV-1 Gag VLPs were shown to improve DC maturation and T-cell priming. These particles efficiently promoted maturation of DCs, increasing the expression of MHC-I and II and costimulatory molecules such as CD80 and CD86. They also induced the natural killer cells in the mice, which are known to play a crucial role in the antitumor response.²⁴ Another study demonstrated that HIV-1 VLPs can propagate innate immune signaling by packaging cGAMP, a messenger that activates antiviral signaling pathways in response to cytosolic sensing of DNA, and delivering it to uninfected target cells.²⁵ On the other hand, the host may sense the invading viral protein via pattern recognition receptors (PRRs) that recognize PAMPs. The HIV-1 capsid can be detected via cyclophilin A and TRIM5 receptors, activating innate immune signaling pathways and subsequent DC maturation.^{26,27} It was also found that the p17 and p24 domains of the HIV-1 Gag protein serve as PAMPs for TLR2 heterodimers,²⁸ significantly increasing the innate immune activation. Agonists of TLR2 and TLR3 are promising adjuvants for vaccine immunotherapy of cancer, to safely enhance antitumor immunity.²⁹

Second, we demonstrated that EP as a delivery method used for DNA vaccination induced innate immunity. Indeed, EP of a pDNA led to the induction of type I IFNs *in vivo*, whereas EP without pDNA or injection of pDNA without EP did not strongly induce the IFN- β promoter (Figure 2). An explanation of this phenomenon may be an increase in DNA plasmid transfection⁷ and thus a higher sensing of aberrant cytosolic DNA. In most cases, the recognition of cytosolic DNA results in the induction of the innate immune response through the STING–TBK1 signaling cascade, and thus the subsequent expression of type I IFNs.¹³ These cytokines play a crucial role in the induction of a protective antitumor immune response.²¹ Adjuvant properties of EP had already been highlighted previously in a series of studies, showing its capacity to trigger a 100-fold increase of antigen expression⁷ but also to recruit DCs to the vaccinated area and induce local tissue inflammation.^{1,10} Here, we reported a direct induction of type I IFNs by EP *in vivo*, which is shown for the first time to our knowledge. This result supports the crucial role of using EP in DNA vaccination protocols to further enhance the immune response against DNA vaccine-encoded antigens.

Then, the potential of pGag to act as an adjuvant in the context of DNA vaccine EP was investigated. Initial evidence of pGag's adjuvant potential came from the analysis of the adaptive immune response triggered by the anti-OVA DNA vaccination. The codelivery of pGag led to a clear shift of the anti-OVA immune response toward a Th1 polarization. This finding was characterized both by a decrease in the total anti-OVA IgG titers and an increase in the IgG2a/IgG1 ratio, as well as an increase in antigen-specific IFN- γ levels in the presence of pGag and an improved induction of antigen-specific CTLs (Figure 3). This regulation of the Th1/Th2 homeostasis driven by pGag favored the cellular immunity and is therefore more likely to induce efficient elimination of cancerous cells.³⁰ pGag's ability to increase DNA vaccine

potency was further proven as it increased protection against tumor challenge. The prophylactic immunization of mice with an anti-OVA DNA vaccine slowed down the growth of B16F10-OVA tumors and improved mouse survival when the antigenic plasmid was combined with pGag (Figure 4). Moreover, the efficacy of this strategy was confirmed in a less immunogenic TAA model by combining pGag with a vaccine coding for the gp100 melanoma antigen. The results indicated that mice developed a more potent immune response to the B16F10-OVA tumor only when pGag was codelivered with pGP100 (Figure 5). In this case, the delivery of the pGP100 encoding plasmid alone did not offer tumor protection, highlighting again the importance of the adjuvant plasmid in inducing an effective immune response. Finally, therapeutic immunization of the mice was tested with the anti-OVA DNA vaccine model. Once again, tumor growth delay was observed only with the combination of antigenic and adjuvant plasmids (Figure 6). These results demonstrated the ability of pGag to regulate adaptive immunity, as the addition of this plasmid promotes a Th1 immune response and, in a consistent way, improves the protective immunity against tumors.

Finally, the mechanisms lying behind the immune modulation induced by pGag were further studied. First of all, the improved vaccine efficacy was specific to pGag codelivery and not due to an increase of DNA amount used for immunizations. Indeed, using 1 μ g or 10 μ g of pOVA DNA vaccine led to similar protection efficacy following B16F10-OVA challenge (see Supplementary Figure S1). As pGag adjuvant effect could be driven by the formation of VLPs *in vivo*, the requirement of particles formation was analyzed. Immunization of mice with a plasmid encoding a mutated form of the HIV-1 Gag protein that prevents VLP formation²² led to similar results than immunization with the plasmid coding for the native protein (Figures 7 and 8). This suggests that the adjuvant effect is probably mediated by immune recognition of the DNA or protein sequence of HIV-1 Gag rather than by VLPs. For instance the HIV-1 Gag plasmid may contain CpG motifs that can be recognized by the TLR9 and activate innate immunity.³¹ About HIV-1 Gag protein, some of its domains were shown to act as PAMPs^{26–28} and induce innate immunity. In addition, the protein may contain MHC-II restricted epitopes that can induce a strong T-helper response.³² The antitumor effect is mediated by the antigen-specific response, as delivery of pGag alone did not offer protection against tumor challenge after prophylactic immunization (Figure 8c). Interestingly, pGag seemed to have an antitumor effect by itself in therapeutic vaccination setting (Figure 7c). This supports the important role played by pGag on immune system mediators. Future work may aim at better characterizing the mechanisms involved.

Taken together, these results support an adjuvant role for pGag when codelivered by EP with a tumor antigen encoding plasmid. This strategy seemed to efficiently stimulate innate immunity, taking advantage of both the ability of DNA EP to stimulate innate immunity and of the immunomodulatory effects induced by pGag. This approach led to an efficient priming of an adaptive immune response and allowed for the augmentation of cancer DNA vaccine efficacy.

The use of pGag as a genetic adjuvant is of particular interest from a translational point of view. Indeed, genetic adjuvants

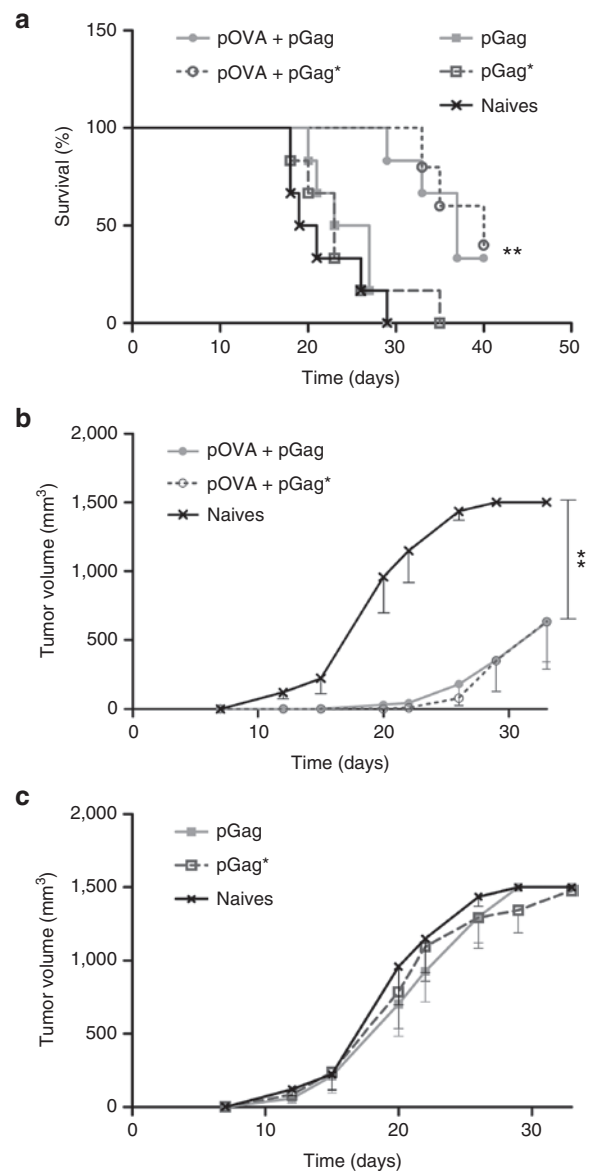


Figure 8 Comparison of the effect of pGag and pGag* during prophylactic anti-ovalbumin (OVA) immunization on the antitumor activity. **(a)** Survival rate monitoring after challenge. The asterisks indicate significant differences compared with naive mice (** $P < 0.01$) (comparison of survival curves, Mantel–Cox test). **(b,c)** Tumor growth follow-up after challenge in mice immunized respectively with pOVA combined with pGag or pGag* and mice immunized with pGag or pGag* alone. The results are expressed as mean \pm SEM ($n = 6$). The asterisks show significant differences between groups (** $P < 0.01$) (analysis of variance, Dunnett's *post-hoc* test).

hold a higher potential for enhancing DNA vaccine potency than traditional ones. First, they possess intrinsic adjuvant properties due to their recognition by cytosolic DNA sensors. In addition, both antigens and adjuvants often need to be delivered at the same time to the patient to obtain coordinated priming of the immune response. As the antigenic plasmid of DNA vaccines is not the physical antigen but its coding sequence, it first needs to be expressed in sufficient amounts by the host cells. Because many conventional adjuvants work immediately after injection, their effect might be lower at the time the antigen is present.³³ In contrast, the use of plasmid encoding immunomodulatory proteins

permits the coordinated delivery of antigens and adjuvants, tailoring the immune response to the demands of each particular disease.⁷ Until now, most of the genetic adjuvants used in trials encode proteins that activate innate immune responses directly, such as cytokines, chemokines, signaling or costimulatory molecules. Here, the strategy is different and innovative as pGag most likely induces innate immune responses indirectly, through PAMP recognition by pattern recognition receptors. Last but not least, HIV-1 Gag has already been involved in clinical trials in the context of HIV vaccine development, where it was shown to be safe.¹⁷ Therefore, the transition from preclinical to clinical evaluation of this strategy would be easier.

In conclusion, this study supports the adjuvant effect of plasmid EP *in vivo*. It demonstrates that immunization with pGag favors Th1 immunity against the DNA vaccine-encoded antigen and consistently delays tumor burden. This work highlights the powerful adjuvant potential of pGag for enhancing DNA vaccine potency and opens interesting tracks for the design of new genetic adjuvants that could be used in a clinical setting in an attempt to overcome the current limitations of DNA vaccines in humans.

MATERIALS AND METHODS

Plasmids. Full length and codon-optimized gene sequences (see **Supplementary Materials and Methods**) of HIV-1 Gag, OVA, and human gp100 were designed using GeneOptimizer and obtained by standard gene synthesis from GeneArt (Thermo Fisher Scientific, Waltham, MA). These sequences were subcloned in the pVAX2 vector as previously described.³⁴ A mutant version of the HIV-1 Gag encoding plasmid was obtained by introducing three point mutations (alanine mutations at the residues G₂, W₃₁₆, and M₃₁₇) in the gene sequence using the QuikChange Multi Site-Directed Mutagenesis Kit (Agilent Technologies, Santa Clara, CA) and following the manufacturer's protocol. The primers used were (Primer Name—Primer Sequence) g35c—5'-ccgccaccatggcagctagagcctc-3' for G2A mutation and t976g_g977c_a979g_t980c—5'-caccagcagtgtctgtcgcgcgcttctcactctctgctg-3' for W316A and M317A mutations. The mutated sequence was checked by Sanger DNA sequencing (Beckman Coulter Genomics, Danvers, MA). The plasmids were prepared using the EndoFree Plasmid Giga Kit (Qiagen, Venlo, Netherlands) according to the manufacturer's protocol. Plasmid dilutions were performed in Dulbecco's PBS (1×) (Life Technologies, Carlsbad, CA). The quality of the purified plasmid was assessed by the ratio of optical densities (260 nm/280 nm) and by 0.5% agarose gel *electrophoresis*. DNA concentration was determined by optical density at 260 nm. The plasmids were stored at -20 °C.

Cell culture. B16F10-OVA, a melanoma cell line from C57BL/6 mice that stably expresses OVA, was cultured in MEM medium supplemented with GlutaMAX with 10% fetal bovine serum, 100 µg/ml streptomycin, and 100 U/ml penicillin (Life Technologies).

HEK 293 T cells were grown in complete DMEM medium supplemented with GlutaMAX (with 10% fetal bovine serum, 2 mmol/l l-Glutamine, 100 µg/ml streptomycin, and 100 U/ml penicillin) (Life Technologies).

VLP production. In total, 3 × 10⁶ HEK 293 T cells were cultured for 2 days in T75 flasks (Sigma-Aldrich, St. Louis, MO) and then transfected with Lipofectamine 2000 following the manufacturer's instructions (Invitrogen, Carlsbad, CA). Seventeen micrograms of pGag and 58 µl of lipofectamine were used for lipofection. The medium was replaced 24 hours after transfection, and the supernatants were collected at days 2, 3, and 4 posttransfection. Cellular debris was removed by low-speed centrifugation and by filtration through a 0.45 µm filter. Filtered supernatants were then ultracentrifuged (50,000g, 2.5 hours, 4 °C) through 20% sucrose. Purified VLPs

were suspended in 50 µl PBS, stored at 4 °C overnight, and placed at -80 °C for long-term storage. The total protein content of each preparation was determined by a Micro BCA assay according to the manufacturer's instruction (Thermo Fisher Scientific).

VLP characterization. Particle size distribution was determined by dynamic light scattering using a NanoSizer ZS (Malvern Instruments, Malvern, UK). Purified samples were diluted 80 times in PBS, and the measurement was performed in triplicate. The data were analyzed using the Dispersion Technology Software 5.00. For particle imaging by transmission electron microscopy, the samples were adsorbed onto 400 mesh formvar-coated EM grids (Ted Pella, Redding, CA) for 10 minutes and then washed three times with distilled water. Excess liquid was removed using filter paper, and the negative contrast was obtained by applying 2% phosphotungstic acid (Sigma-Aldrich) at pH 7 for 2 minutes. The grids were air dried for 10 minutes and then examined in a LEO 922 electron microscope with a CCD camera. Western blot analyses were performed on 10 µg of protein from the purified VLP samples. The proteins were denatured in 2× Laemmli Sample Buffer for 7 minutes at 95 °C. After loading the samples on a Mini-PROTEAN TGX Precast Gels 4–20% (Bio-Rad, Hercules, CA), electrophoresis was performed at 300 V for 15 minutes using a 1% Tris-glycin-0.1% sodium dodecyl sulfate running buffer (Sigma-Aldrich). The proteins were then transferred to a nitrocellulose membrane using the trans-Blot Turbo Transfer System following the manufacturer's instruction (Bio-Rad). After blocking, primary rabbit polyclonal antibodies to HIV-1 Gag and OVA (Fitzgerald, Acton, MA) were added, all diluted 1:2,000, for an hour. Biotinylated anti-rabbit secondary antibodies (Vector Laboratories, Cambridge, UK) at 1:1,000 were added for 1 hour and followed by streptavidin-horseradish peroxidase for 20 minutes. Visualization was performed with a 50:50 ECL Western Blotting Substrate and SuperSignal West Femto Maximum Sensitivity Substrate solution (Thermo Scientific).

Animals. Six-week-old C57BL/6 female mice were obtained from Janvier Labs (Le Genest Saint Isle, France) and housed in a minimal disease facility with *ad libitum* access to food and water. For the immunization studies, the mice were 7 weeks old at the beginning of the experiments. For tumor implantation and EP, the mice were anesthetized by intraperitoneal (i.p.) injection of 150 µl of a solution of 10 mg/ml ketamine and 1 mg/ml xylazine. Heterozygous luciferase reporter mice (IFN-β+/Δβ-luc) with a BALB/c background were bred with *ad libitum* access to food and water. Male and female mice were aged 12 weeks at the beginning of the experiments. For imaging, the mice were anesthetized by isoflurane (Abbott Animal Health; Medini NV). The ethical committee for Animal Care and Use of the Medical Sector of the Université Catholique de Louvain approved our experimental protocols (UCL/MD/2011/007).

Type 1 IFN induction: in vivo bioluminescence imaging. Heterozygous luciferase reporter mice were anesthetized by i.p. injection of 150 µl of a solution of 10 mg/ml ketamine and 1 mg/ml xylazine. After removing the hair using a rodent shaver (AgnTho's, Lidingö, Sweden), the left tibial cranial muscle was injected with 30 µl of PBS or 30 µl of empty plasmid DNA solution diluted in PBS. This injection was followed or not by EP. For EP, a conductive gel was applied on the leg to ensure electrical contact with the skin (EKO-GEL, ultrasound transmission gel, Egna, Italy) and eight 20 ms and 200 V/cm electrical pulses were delivered through 4 mm spaced plate electrodes by a Cliniporator system with a frequency of 2 Hz (Cliniporator, IGEA, Carpi, Italy). For *in vivo* bioluminescence imaging, the mice were injected i.p. with 150 mg/kg of VivoGlo luciferin (Promega, Fitchburg, WI) in PBS and monitored using an IVIS Lumina II imaging system. Photon flux was quantified using the Living Image 4.4 software (all from Perkin Elmer, Waltham, MA).

Mouse immunization. C57BL/6 mice were shaved, and their left tibial cranial muscle was injected with a plasmid DNA solution. The solutions

were composed of 1 µg or 50 µg of antigenic OVA or GP100 plasmid alone or with 1 µg HIV-1 Gag encoding plasmid. One microgram of a plasmid coding for a mutated form of HIV-1 Gag was also used for immunization, combined or not with 1 µg of pOVA. A conductive gel was applied, and EP was performed as previously described. The plasmids were administered three times, every week or every 2 weeks for therapeutic and prophylactic DNA immunization, respectively.

Tumor implantation and tumor growth measurement. In total, 1×10^5 B16F10-OVA cells diluted in 100 µl PBS were injected subcutaneously into the right flank of each C57BL/6 mouse 2 days before the first plasmid administration or 2 weeks after the last administration for therapeutic and prophylactic DNA immunization studies, respectively. The tumor size was measured three times a week with an electronic digital calliper. Tumor volume was calculated as the length \times width \times height (in mm³). The mice were sacrificed when the volume of the tumor reached 1,500 mm³ or when they were in poor condition and expected to die shortly.

Immunoglobulin titers. Ten days after the last plasmid administration, blood samples were collected and sera were isolated by centrifugation at 3,700g for 15 minutes at 4 °C and stored at -20 °C until use. OVA-specific IgG, IgG1, and IgG2a levels were determined by enzyme-linked immunosorbent assay as previously described.³⁵ Briefly, OVA was coated on Nunc Maxisorp plates. Several sera dilutions were made, and the detection of anti-OVA antibodies was performed using peroxidase-labeled rat anti-mouse immunoglobulin G, G1, and G2a (LO-IMEX, Brussels, Belgium). IgG titers were defined as the logarithm of the inverse of the sera dilution corresponding to an absorbance equal to the blank value plus 10 times the standard deviation.

Antigen-specific IFN-γ levels. Mice were immunized and killed 2 weeks after the third vaccine administration. The spleens were removed aseptically, and splenocytes were isolated as previously described.³⁶ Then, 96-well plates were seeded with 1×10^6 cells in 100 µl of media per well. The cells were stimulated by adding 100 µl of 100 µg/ml of OVA solution (Sigma-Aldrich). The plates were incubated at 37 °C in a humidified incubator at 5% CO₂. The supernatants were collected after 24, 48, and 72 hours of restimulation, and cytokine production was assessed using DuoSet ELISA Development kits for IFN-γ (R&D Systems, Abingdon, UK) according to the manufacturer's instructions. The concentrations, expressed in pg/ml, were determined by reference to cytokine standard curves.

In vivo cytotoxicity assay. Splenocytes from female C57BL/6 mice were pulsed with 1 µg/ml of MHC-I OVA peptide or MHC-I gp100 peptide (Anaspec) before labeling with 5 µmol/l (hi) or 0.5 µmol/l (low) CFSE (Invitrogen, Merelbeke, Belgium), respectively. Labelled cells were mixed at a 1:1 ratio, and a total of 1×10^7 cells were adoptively transferred into the immunized mice. Two days after transfer, the spleens of the host mice were isolated and analyzed by flow cytometry after staining with α-F4/80 (BD Biosciences, San Diego, CA) to exclude auto-fluorescent macrophages. The percentage antigen-specific killing was determined using the following formula: $100 - 100 \times ((\% \text{ CFSE}^{\text{hi}} \text{ cells} / \% \text{ CFSE}^{\text{low}} \text{ cells})^{\text{immunized mice}} / (\% \text{ CFSE}^{\text{hi}} \text{ cells} / \% \text{ CFSE}^{\text{low}} \text{ cells})^{\text{nonimmunized mice}})$.³⁷

Statistical analysis. The results are presented as the means \pm SEM. The differences in means between groups were analyzed for significance using appropriate tests (GraphPad Prism Software). Nonparametric tests were used to study type I IFN induction, antibody titers, INF-γ concentration, and OVA-peptide-pulsed-target cells specific killing as four to six mice per group were used in those experiments. Survival curves were compared via Mantel-Cox (log-rank) test. Finally, repeated measures analysis of variance was applied for B16F10-OVA tumor growth analysis, assuming Gaussian distribution of the data for that tumor model.

SUPPLEMENTARY MATERIAL

Figure S1. The effect of pOVA dose during prophylactic anti-OVA immunization on the antitumor activity. Supplementary Materials and Methods

ACKNOWLEDGMENTS

L.L. is a research fellow and G.V. is a postdoctoral researcher of the Fonds de la Recherche Scientifique-FNRS, Belgium. The authors would like to thank Sabrina El Bachiri for her help with the statistical analysis. N.N.S. acknowledges funding from Research Fund—Flanders (FWO, grant no. G.0621.10) and Bijzonder Onderzoeksfonds (BOF) from Ghent University. The authors declare no conflict of interest.

REFERENCES

- Calvet, CY, Andre, FM and Mir, LM (2014). Dual therapeutic benefit of electroporation-mediated DNA vaccination in vivo: enhanced gene transfer and adjuvant activity. *Oncoimmunology* **3**: e28540.
- Donnelly, JJ, Wahren, B and Liu, MA (2005). DNA vaccines: progress and challenges. *J Immunol* **175**: 633–639.
- Braumüller, H, Wieder, T, Brenner, E, Aßmann, S, Hahn, M, Alkhaled, M *et al.* (2013). T-helper-1-cell cytokines drive cancer into senescence. *Nature* **494**: 361–365.
- Rosenberg, SA, Yannelli, JR, Yang, JC, Topalian, SL, Schwartzentruber, DJ, Weber, JS *et al.* (1994). Treatment of patients with metastatic melanoma with autologous tumor-infiltrating lymphocytes and interleukin 2. *J Natl Cancer Inst* **86**: 1159–1166.
- Castellino, F and Germain, RN (2006). Cooperation between CD4+ and CD8+ T cells: when, where, and how. *Annu Rev Immunol* **24**: 519–540.
- Senovilla, L, Vacchelli, E, Garcia, P, Eggmont, A, Fridman, WH, Galon, J *et al.* (2013). Trial watch: DNA vaccines for cancer therapy. *Oncoimmunology* **2**: e23803.
- Flingai, S, Czerwonko, M, Goodman, J, Kudchodkar, SB, Muthumani, K and Weiner, DB (2013). Synthetic DNA vaccines: improved vaccine potency by electroporation and co-delivered genetic adjuvants. *Front Immunol* **4**: 354.
- Lambrecht, L, Lopes, A, Kos, S, Sersa, G, Prétat, V and Vandermeulen, G (2016). Clinical potential of electroporation for gene therapy and DNA vaccine delivery. *Expert Opin Drug Deliv* **13**: 295–310.
- Babiuk, S, Baca-Estrada, ME, Foldvari, M, Storms, M, Rabussay, D, Widera, G *et al.* (2002). Electroporation improves the efficacy of DNA vaccines in large animals. *Vaccine* **20**: 3399–3408.
- Chiarella, P, Massi, E, De Robertis, M, Sibilio, A, Parrella, P, Fazio, VM *et al.* (2008). Electroporation of skeletal muscle induces danger signal release and antigen-presenting cell recruitment independently of DNA vaccine administration. *Expert Opin Biol Ther* **8**: 1645–1657.
- Clark, R and Kupper, T (2005). Old meets new: the interaction between innate and adaptive immunity. *J Invest Dermatol* **125**: 629–637.
- Scheerlinck, JY (2001). Genetic adjuvants for DNA vaccines. *Vaccine* **19**: 2647–2656.
- Kobiyama, K, Jounai, N, Aoshi, T, Tozuka, M, Takeshita, F, Coban, C *et al.* (2013). Innate immune signaling by, and genetic adjuvants for DNA vaccination. *Vaccines (Basel)* **1**: 278–292.
- Li, L, Saade, F and Petrovsky, N (2012). The future of human DNA vaccines. *J Biotechnol* **162**: 171–182.
- Kelleher, AD, Puls, RL, Bebbington, M, Boyle, D, Ffrench, R, Kent, SJ *et al.* (2006). A randomized, placebo-controlled phase I trial of DNA prime, recombinant fowlpox virus boost prophylactic vaccine for HIV-1. *AIDS* **20**: 294–297.
- Jin, X, Morgan, C, Yu, X, DeRosa, S, Tomaras, GD, Montefiori, DC *et al.*; NIAID HIV Vaccine Trials Network. (2015). Multiple factors affect immunogenicity of DNA plasmid HIV vaccines in human clinical trials. *Vaccine* **33**: 2347–2353.
- Kalams, SA, Parker, S, Jin, X, Elizaga, M, Metch, B, Wang, M *et al.*; NIAID HIV Vaccine Trials Network (2012). Safety and immunogenicity of an HIV-1 Gag DNA vaccine with or without IL-12 and/or IL-15 plasmid cytokine adjuvant in healthy, HIV-1 uninfected adults. *PLoS One* **7**: e29231.
- Gottlinger, H (2001). HIV-1 Gag: a molecular machine driving viral particle assembly and release. Theoretical Biology and Biophysics Group, Los Alamos National Laboratory, Los Alamos, NM, LA-UR, 02-28.
- Melchjorsen, J (2013). Learning from the messengers: innate sensing of viruses and cytokine regulation of immunity—clues for treatments and vaccines. *Viruses* **5**: 470–527.
- Vandermeulen, G, Athanasopoulos, T, Trundle, A, Foster, K, Prétat, V, Yáñez-Muñoz, RJ *et al.* (2012). Highly potent delivery method of gp160 envelope vaccine combining lentivirus-like particles and DNA electrotransfer. *J Control Release* **159**: 376–383.
- Rizza, P, Moretti, F, Capone, I and Belardelli, F (2015). Role of type I interferon in inducing a protective immune response: perspectives for clinical applications. *Cytokine Growth Factor Rev* **26**: 195–201.
- O'Carroll, IP, Crist, RM, Mirro, J, Harvin, D, Soheilian, F, Kamata, A *et al.* (2012). Functional redundancy in HIV-1 viral particle assembly. *J Virol* **86**: 12991–12996.
- Bachmann, MF and Jennings, GT (2010). Vaccine delivery: a matter of size, geometry, kinetics and molecular patterns. *Nat Rev Immunol* **10**: 787–796.
- Chang, MO, Suzuki, T, Suzuki, H and Takaku, H (2012). HIV-1 Gag-virus-like particles induce natural killer cell immune responses via activation and maturation of dendritic cells. *J Innate Immun* **4**: 187–200.
- Gentili, M, Kowal, J, Tkach, M, Satoh, T, Lahaye, X, Conrad, C *et al.* (2015). Transmission of innate immune signaling by packaging of cGAMP in viral particles. *Science* **349**: 1232–1236.
- Manel, N, Hogstad, B, Wang, Y, Levy, DE, Unutmaz, D and Littman, DR (2010). A cryptic sensor for HIV-1 activates antiviral innate immunity in dendritic cells. *Nature* **467**: 214–217.

27. Pertel, T, Hausmann, S, Morger, D, Züger, S, Guerra, J, Lascano, J *et al.* (2011). TRIM5 is an innate immune sensor for the retrovirus capsid lattice. *Nature* **472**: 361–365.
28. Henrick, BM, Yao, XD and Rosenthal, KL; INFANT study team (2015). HIV-1 structural proteins serve as PAMPs for TLR2 heterodimers significantly increasing infection and innate immune activation. *Front Immunol* **6**: 426.
29. Seya, T, Shime, H, Takeda, Y, Tatematsu, M, Takashima, K and Matsumoto, M (2015). Adjuvant for vaccine immunotherapy of cancer—focusing on Toll-like receptor 2 and 3 agonists for safely enhancing antitumor immunity. *Cancer Sci* **106**: 1659–1668.
30. Kidd, P (2003). Th1/Th2 balance: the hypothesis, its limitations, and implications for health and disease. *Altern Med Rev* **8**: 223–246.
31. Ohlschläger, P, Spies, E, Alvarez, G, Quetting, M and Groettrup, M (2011). The combination of TLR-9 adjuvantation and electroporation-mediated delivery enhances *in vivo* antitumor responses after vaccination with HPV-16 E7 encoding DNA. *Int J Cancer* **128**: 473–481.
32. Paul, S and Piontkivska, H (2010). Frequent associations between CTL and T-helper epitopes in HIV-1 genomes and implications for multi-epitope vaccine designs. *BMC Microbiol* **10**: 212.
33. Grunwald, T and Ulbert, S (2015). Improvement of DNA vaccination by adjuvants and sophisticated delivery devices: vaccine-platforms for the battle against infectious diseases. *Clin Exp Vaccine Res* **4**: 1–10.
34. Vandermeulen, G, Uyttendrove, C, De Plaen, E, Van den Eynde, BJ and Pr at, V (2014). Intramuscular electroporation of a P1A-encoding plasmid vaccine delays P815 mastocytoma growth. *Bioelectrochemistry* **100**: 112–118.
35. Garinot, M, Fi vez, V, Pourcelle, V, Stoffelbach, F, des Rieux, A, Plapied, L *et al.* (2007). PEGylated PLGA-based nanoparticles targeting M cells for oral vaccination. *J Control Release* **120**: 195–204.
36. Silva, JM, Zupancic, E, Vandermeulen, G, Oliveira, VG, Salgado, A, Videira, M *et al.* (2015). *In vivo* delivery of peptides and Toll-like receptor ligands by mannose-functionalized polymeric nanoparticles induces prophylactic and therapeutic anti-tumor immune responses in a melanoma model. *J Control Release* **198**: 91–103.
37. De Geest, BG, Willart, MA, Lambrecht, BN, Pollard, C, Vervae, C, Remon, JP *et al.* (2012). Surface-engineered polyelectrolyte multilayer capsules: synthetic vaccines mimicking microbial structure and function. *Angew Chem Int Ed Engl* **51**: 3862–3866.